Suppressive Interactions between Nearby Stimuli in Visual Cortex Reflect Crowding

Leili Soo[1], Plamen A. Antonov[2], Ramakrishna Chakravarthi[2] and Søren K. Andersen[2,3]

Abstract

■ Crowding is a phenomenon in which visual object identification is impaired by the close proximity of other stimuli. The neural processes leading to object recognition and its breakdown as seen in crowding are still debated. To assess how crowding affects the processing of stimuli in visual cortex, we recorded steady-state visual evoked potentials (SSVEPs) elicited by flickering target and flanker stimuli while manipulating the spacing of these stimuli (Experiment 1) as well as target similarity (Experiment 2). Participants who performed an orientation discrimination task while proportion correct, along with frequency-tagged SSVEPs elicited by target and flanker stimuli, were recorded. Decreasing target–flanker distance reduced both behavioral performance and target-elicited SSVEP amplitudes. Estimates of the critical spacing, a measure of the spatial extent of crowding, from both behavioral data and SSVEP amplitudes were similar. In addition, manipulating target similarity affected both measures in the same way. These findings establish a clear connection between the suppression of stimulus processing by nearby flankers in visual cortex and crowding, and demonstrate the usefulness of SSVEPs in studying the cortical mechanisms of visual crowding. ■

INTRODUCTION

Visual crowding occurs when objects that are easily recognizable in isolation become difficult to identify in clutter (Strasburger, Rentschler, & Jüttner, 2011; Andriessen & Bouma, 1976; Bouma, 1970). Because everyday visual scenes are filled with diverse and complex information, crowding affects us at all times and poses a fundamental limit to object recognition (Whitney & Levi, 2011; Levi, 2008). Despite decades of extensive research on crowding, its underlying neural mechanisms remain unclear. Gaining a clearer understanding of these mechanisms would allow for the integration of behavioral and neurophysiological perspectives, helping to create a more comprehensive view of how visual information is processed from initial sensory input to final perceptual experience.

The primary manifestation of crowding is spatial interference: The closer the flanking objects are to the target, the worse the ability to recognize the target (Toet & Levi, 1992; Bouma, 1970). This spatial interference is typically measured by critical spacing, the minimum distance beyond which flankers cease to interfere with target processing (Pelli, Palomares, & Majaj, 2004; Toet & Levi, 1992; Bouma, 1970). Critical spacing varies depending on various factors (Soo, Chakravarthi, & Andersen, 2018). One such factor that is known to reduce the critical spacing is target–flanker dissimilarity (or "pop-out"), whereby a target ungroups from flankers via a featural singleton, such as in shape, polarity, orientation, depth, or color (Yashar, Chen, & Carrasco, 2015; Kennedy & Whitaker, 2010; Chakravarthi & Cavanagh, 2007; Põder & Wagemans, 2007; Scolari, Kohnen, Barton, & Awh, 2007; Chung, Levi, & Legge, 2001; Kooi, Toet, Tripathy, & Levi, 1994; Nazir, 1992; Andriessen & Bouma, 1976). Similarly, critical spacing is reduced when flankers are previewed, that is, displayed before target onset (Soo et al., 2018; Scolari et al., 2007; Watson & Humphreys, 1997), backward-masked (Wallis & Bex, 2011; Chakravarthi & Cavanagh, 2009), or the target location is precued (Kewan-Khalayly, Migó, & Yashar, 2022; Kewan-Khalayly & Yashar, 2022; Albonico, Martelli, Bricolo, Frasson, & Daini, 2018; Strasburger & Malania, 2013; Yeshurun & Rashal, 2010; Scolari et al., 2007). The extent of crowding is larger when flankers have a higher contrast compared with targets (Soo et al., 2018; Rashal & Yeshurun, 2014) or if targets are backward-masked (Vickery, Shim, Chakravarthi, Jiang, & Luedeman, 2009). Critical spacing can also be decreased with longer display durations or increased with shorter ones (Soo et al., 2018; Tripathy, Cavanagh, & Bedell, 2014; Tripathy & Cavanagh, 2002; Kooi et al., 1994). An important exception to spatial proximity being central to or determinant of crowding occurs when the target ungroups from the flankers, alleviating or even eliminating the crowding effect (Herzog & Sayim, 2022; Herzog, Sayim, Chicherov, & Manassi, 2015; Manassi, Sayim, & Herzog, 2012, 2013; Saarela, Westheimer, & Herzog, 2010; Malania, Herzog, & Westheimer, 2007).

[1]Miguel Hernandez University of Elche Institute of Bioengineering, [2]University of Aberdeen, [3]Syddansk Universitet Institut for Psykologi

https://doi.org/10.1162/JOCN.a.79

Such behavioral observations have inspired several theories to account for them (Manassi & Whitney, 2018; Strasburger et al., 2011; Whitney & Levi, 2011; Levi, 2008). These include proposals such as spatial pooling, where visual information is integrated over some area (Greenwood, Bex, & Dakin, 2009; Pelli et al., 2004; Wilkinson, Wilson, & Ellemberg, 1997); substitution, where features from distractors or entire distractor objects are erroneously attributed to the target or mislocalized (Strasburger & Malania, 2013; Nandy & Tjan, 2007; Levi, Klein, & Yap, 1987; Levi & Klein, 1986); grouping of nearby visual elements (Manassi et al., 2012); and limitations in attentional resources (Intriligator & Cavanagh, 2001). These theories, although hinting at possible neural processes, cannot pinpoint the specific neural mechanisms responsible for crowding.

Neurophysiological approaches, including fMRI, EEG, and magnetoencephalography, attempt to address the neural mechanisms directly. Although the spacing of photoreceptors in the retina are hardwired and impose a physical bottleneck on the richness of detail that can be perceived (Hirsch & Curcio, 1989), the spatial scale of interference seen in crowding is larger than can be accounted for by this sensory bottleneck (Chung & Tjan, 2007; Danilova & Bondarko, 2007; Tripathy & Levi, 1994; Flom, Heath, & Takahashi, 1963). Crowding likely occurs in multiple areas along the visual hierarchy (Anderson, Dakin, Schwarzkopf, Rees, & Greenwood, 2012), from early visual cortical regions like V1 and V2 (He, Wang, & Fang, 2019; Chen et al., 2014; Millin, Arman, Chung, & Tjan, 2014) to mid-level areas like V4 (Kim & Pasupathy, 2024) or lateral occipital cortex (Chicherov, Plomp, & Herzog, 2014), and possibly even higher-order regions in inferotemporal cortex (Jehee, Roelfsema, Deco, Murre, & Lamme, 2007). The exact location and nature of interference processes can vary depending on the specific characteristics of the stimuli and the spatial context in which they are presented. There are proposals of fixed interference zones at a cortical level (Pelli, 2008; Pelli & Tillman, 2008); however, this explanation struggles to account for the large variations in critical spacing that are observed when multiple factors that modulate crowding are combined (Soo et al., 2018).

In crowding, the presence of multiple nearby stimuli imposes a bottleneck on the visual system's processing resources. This type of situation is prototypical of conditions that attention is supposed to help resolve by focusing on the most relevant stimuli. Indeed, neurophysiological studies of attention have investigated interference between nearby stimuli and found mutually suppressive interactions between them in visual cortex using macaque single unit recordings (Luck, Chelazzi, Hillyard, & Desimone, 1997; Moran & Desimone, 1985), human fMRI (Beck & Kastner, 2005; Kastner & Ungerleider, 2001; Kastner, De Weerd, Desimone, & Ungerleider, 1998), and human EEG (Keitel, Andersen, Quigley, & Müller, 2013; Keitel, Andersen, & Müller, 2010; Fuchs, Andersen, Gruber, & Müller, 2008). These findings have been integrated in the biased competition model (Desimone, 1998; Desimone & Duncan, 1995) as well as the normalization (Lee & Maunsell, 2009; Reynolds & Heeger, 2009) and neural theory of visual attention (Bundesen, Habekost, & Kyllingsbæk, 2005) models of attention. According to these models, nearby stimuli compete for neuronal representation due to the limited processing capacity of the visual system. This competition is biased toward one or another stimulus based on bottom–up (e.g., stimulus properties such as salience) and top–down factors (e.g., selective attention).

Here, we hypothesize that the spatial pooling invoked to explain crowding (Keshvari & Rosenholtz, 2016; Freeman, Chakravarthi, & Pelli, 2012; Chung et al., 2001) may neuronally be implemented through the competitive interactions between nearby stimuli described in models of attention (Lee & Maunsell, 2009; Reynolds & Heeger, 2009; Bundesen et al., 2005; Desimone & Duncan, 1995). Although behavioral results in the crowding literature are not often discussed in terms of biased competition models, the latter offer a potential bridge between such behavioral findings and the well-characterized neural mechanisms of attention, thus providing a framework for understanding spatial interference. The putative link between models of attention and visual crowding is supported by previous attempts to connect crowding to attention (Chakravarthi & Cavanagh, 2007; Intriligator & Cavanagh, 2001; He, Cavanagh, & Intriligator, 1996) and also by observations that cueing spatial attention to target locations reduces crowding (Kewan-Khalayly et al., 2022; Kewan-Khalayly & Yashar, 2022; Albonico et al., 2018; Strasburger & Malania, 2013; Yeshurun & Rashal, 2010; Scolari et al., 2007). If this hypothesis is true, suppression of target processing in visual cortex by flankers should exhibit similar patterns as behavioral measures of crowding. Note that suppression of target processing by nearby flankers is not unique to the biased competition model but also proposed by some theories of crowding (Chicherov & Herzog, 2015; Chen et al., 2014). We are not positing that the observation of target suppression in visual cortex will exclusively support the biased competition model of competition (or its extensions) as a framework for understanding crowding, but that such observations would provide important links between crowding and the extensive and well-established neural framework of biased competition models and thereby present an avenue for developing a deeper understanding of neural processes underlying crowding.

To separate cortical processing of concurrently presented target and flanker stimuli from each other, we recorded "frequency-tagged" steady-state visual evoked potentials (SSVEPs). A stimulus flickering at a specific frequency drives a cortical response at the same temporal frequency (Adrian & Matthews, 1934) that can be recorded noninvasively using EEG. When flickering multiple stimuli at different frequencies, each of them drives an SSVEP response at its specific frequency allowing for a concurrent

and continuous measurement of the visual processing of all these stimuli. This method has been utilized in many areas of vision science (reviewed by Norcia, Appelbaum, Ales, Cottereau, & Rossion, 2015) and has proven particularly powerful in studying visual attention (Adamian & Andersen, 2024; Andersen, Müller, & Hillyard, 2012; Morgan, Hansen, & Hillyard, 1996). To date, SSVEPs have been employed to investigate crowding only once, showing a crowding-induced suppression of target-elicited SSVEP amplitudes (Chicherov & Herzog, 2015) by nearby flankers, which is reduced by target–distracter dissimilarity. However, this study did not manipulate the spatial separation between stimuli and hence could not assess the relationship between spatial interactions at the behavioral and neural levels. Other studies have investigated suppression of stimulus processing from nearby flanker stimuli using SSVEPs (Keitel et al., 2010, 2013; Fuchs et al., 2008); however, the behavioral data in these studies cannot readily be related to crowding and none of these articles attempted to relate their findings to crowding. Thus, the exact relationship between suppressive stimulus interactions in visual cortex and crowding remains unclear.

In two experiments, we investigated how closely the neural suppression between nearby stimuli reflects the behavioral effects of crowding. We manipulated target–flanker distance (Experiments 1 and 2) and similarity (Experiment 2) while recording frequency-tagged SSVEPs from flickering target and flanker stimuli and behavioral target identification performance. If the recorded SSVEPs capture processes underlying crowding, we would expect corresponding changes in target-elicited SSVEP amplitudes and target identification performance with changes in target–flanker distance and similarity.

METHODS

Participants

We tested 15 participants (10 male, 9 right-handed, mean age = 25 years, age range: 21–36 years) in Experiment 1 and 19 participants (15 female, 3 left-handed, mean age = 21.9 years, age range: 18–29 years) in Experiment 2. Participants gave written informed consent before participation and received £12 or course credits as compensation for their time. All participants reported normal or corrected-to-normal visual acuity and no known visual or neurological disorders. The experiments were approved by the University of Aberdeen Psychology ethics committee (Experiment 1 project number: PEC/3234/2015/6, Experiment 2 project number: PEC/3522/2016/10).

Two participants were excluded from statistical analyses because their performance (proportion correct) in the "No flanker" condition was more than 3 *SD*s below the mean (one in Experiment 1, one in Experiment 2). All participants had at least 50% of all epochs remaining after EEG artifact correction in each condition (71.3% ± 14.1% trials remaining on average in Experiment 1 and 71.4% ± 19.7% in Experiment 2); no participant's data were excluded due to excessive EEG artifacts.

The required sample size was computed using the power calculators provided by Gregory Francis (https://www1.psych.purdue.edu/~gfrancis/calculators/calculators.html), which are based on equations outlined in a textbook (Herzog, Francis, & Clarke, 2019). Our power analysis was based on previous reports of performance in two different settings. (1) The effect of target–flanker distance: Kooi and colleagues (1994) found that with $n = 5$, average percent correct for targets presented at an eccentricity of 10° at various target–flanker distances was 29.8% at 1.25°, 32.8% at 2.5°, 39.8% at 3.75°, 58.8% at 5°, 70.2% at 6.25°, and 97.6% with no flankers; population $SD = 27.3\%$. These data recommended a sample size of three to detect the effect of target–flanker distance with a power of 95%. (2) The effect of similarity on crowding: Kooi and colleagues (1994) found that the mean difference in critical spacing between similar and dissimilar target–flanker conditions ($n = 5$) was −3.18 deg, with an *SD* of 1.51 deg. This yields a standardized effect size of 3.17; hence, we would need a sample size of six to detect the effect of similarity in crowding at a power of 95%. As our study is only the second to investigate crowding using the SSVEP, we had no good prior effect size estimates for the SSVEP effects. Therefore, we opted to test a much larger number of participants than the recommended number ($n = 3$ or 6) to test out hypothesis.

Task and Stimuli

The experiments were created and presented using MATLAB (MathWorks Inc.) with the Cogent Graphics toolbox (John Romaya, Laboratory of Neurobiology, Wellcome Department of Imaging Neuroscience) on a 19-in. CRT monitor with a resolution of 800 × 600 pixels and a refresh rate of 120 Hz, viewed from a distance of 60 cm.

Stimuli and Procedure

Stimuli were displayed for 4000 msec, followed by a 1000 msec intertrial interval (Figure 1). Participants were instructed to fixate a circle presented in the center of the screen and focus bilaterally on target stimuli (four superimposed letter "T"s in four cardinal orientations, 1.4° × 1.4° visual angle) presented at 9° to the left and right of fixation. In separate trials, targets were either presented in isolation or surrounded by four identical flankers (above, below, left, and right of target) at one of the tested flanker distances. In Experiment 1, flankers were presented at seven different center-to-center distance from targets: 1.7°, 2°, 2.5°, 2.9°, 3.5° 4.3°, or 5.1° of visual angle. In Experiment 2, flankers were presented at three different distances: 1.7°, 2.5°, and 5°. In any given trial, all eight flankers were presented at the same distance from the targets. To generate SSVEPs, the left target flickered at 10 Hz, the right target at 12 Hz, and all flankers at 15 Hz with

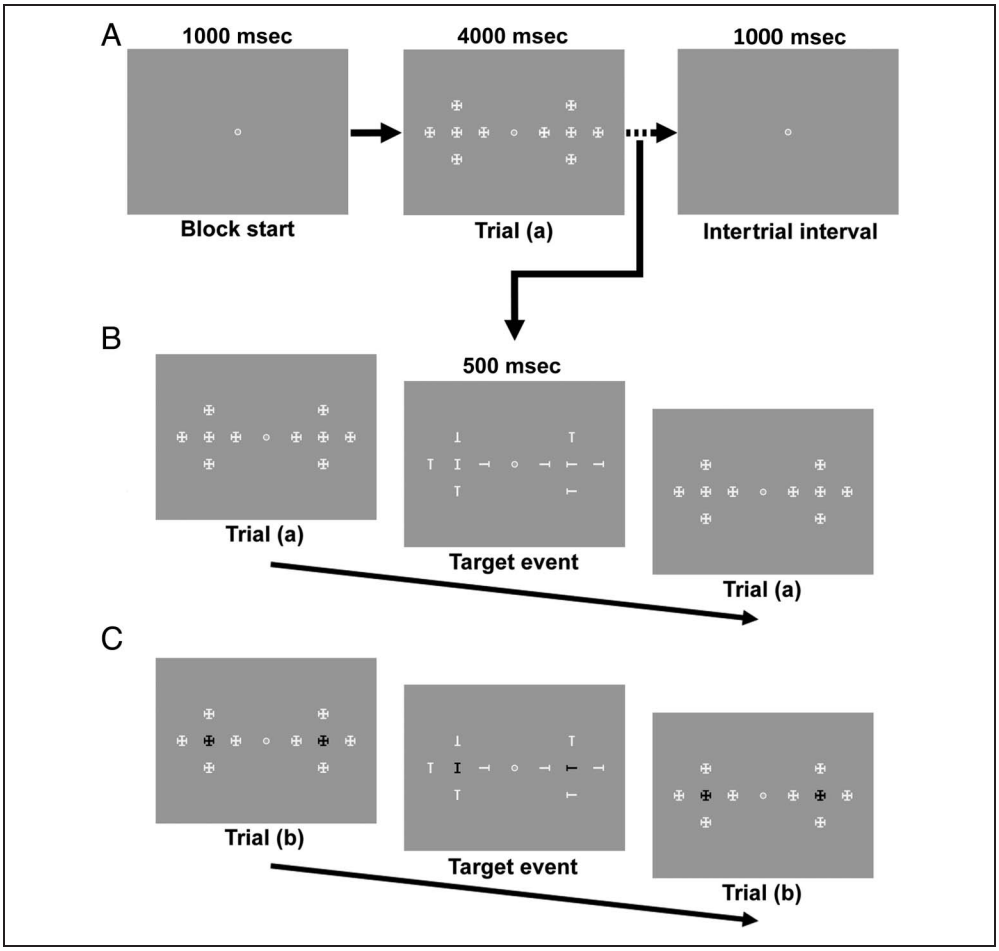

Figure 1. The sequence of events in Experiments 1 and 2. (A) Each block started with a 1000-msec fixation, followed by stimulus presentation for 4000 msec. There was a 200-msec audio feedback within a 1000-msec intertrial interval between two consecutive trials. Participants were instructed to attend to bilateral target locations, where shapes were presented either in isolation or surrounded by four flankers on each side at different target–flanker distances. (B) In two thirds of the trials, there were one to two target events where a letter "I" was presented in one of the target locations and a letter "T" in the other for 500 msec. Participants were instructed to report the orientation of the target letter "T" (up, down, left, or right) as quickly and accurately as possible. Flankers, when presented, were positioned at one of seven (Experiment 1) or three (Experiment 2) center-to-center distances. In Experiment 2, targets and flankers were presented either with the same or opposite contrast polarity (same contrast polarity: A and B; opposite polarity: C). In Experiment 2, the fixation circle was red, isoluminant to the gray background.

synchronous onsets of these stimuli every 500 msec. In Experiment 1, only flanker distance was varied; however, in Experiment 2, targets and flankers were presented either with same or opposite contrast polarity.

Target Events

During some trials, there were brief 500-msec target events (up to two per trial), where one of the shapes at target locations changed into a target letter T (1.4° × 0.5° visual angle) in one of four orientations (up, down, left, or right) and the other into an I letter (vertical or horizontal; 1.4° × 0.5° visual angle). Simultaneously, all flankers turned into letter Ts presented at random orientations (0°, 90°, 180°, and 270°). Participants were instructed to report the orientation of the letter T at target location by pressing the corresponding arrow key, while ignoring the flankers and the letter I. Target event onsets occurred between 1000 and 3500 msec after stimulus display onset, with a minimum of 1500 msec between two target events within a trial. Target events were time-locked to the 500-msec cycles to ensure synchronous onsets of all stimuli.

Stimulus Properties

In Experiment 1, all stimuli (targets, flankers, and fixation circle) had a luminance of 12.47 cd/m^2, and the background was 5.61 cd/m^2. In Experiment 2, the white (positive contrast polarity) stimulus was 11.2 cd/m^2 and the black (negative contrast polarity) stimulus was 0.01 cd/m^2. At fixation in the center of the screen was a red circle, isoluminant to the background (5.61 cd/m^2). The Weber contrast was calculated as follows:

$$contrast = \frac{I - I_b}{I_b} \quad (1)$$

where I is the luminance of the stimulus and I_b is the background luminance, resulting in a contrast of 1.2 in Experiment 1 and ±1 in Experiment 2.

Design

Participants completed between one and three training blocks (20 trials each) to familiarize themselves with the task. In Experiment 1, the main experiment consisted of 576 trials in total (72 trials per condition) divided into eight blocks of 72 trials. In Experiment 2, the main experiment

consisted of 756 trials (54 trials per condition), divided into six blocks of 126 trials. Within each block, the experimental conditions were balanced and repeated nine times. Target events occurred in two thirds of the trials and were randomized to ensure eight events per condition in each block.

Feedback and Breaks

At the end of each trial, participants received auditory feedback (high-pitched beep for correct responses, low-pitched beep for incorrect or missed responses). After each block, participants were shown their average accuracy. They were allowed a self-paced break between blocks.

EEG Procedure

During the experiment, participants sat in a dark electrically shielded chamber. Participants were instructed to try to blink as little as possible, maintain central fixation, and sit still with relaxed muscles. Electrophysiological data were recorded from 64 scalp electrodes mounted on an elastic cap and six additional electrodes (HEOG and VEOG and earlobes) using a BioSemi Active-Two amplifier system. Scalp electrodes were positioned according to the International 10–20 system (Klem, Lüders, Jasper, & Elger, 1999), with electrodes Common Mode Sense and Driven Right Leg serving as reference and ground during the recording (see https://www.biosemi.com/faq/cms&drl.htm). We used a modified 64-electrode channel layout that omitted electrode positions F5, F6, C7, and C8 in exchange for I1, I2, PO09, and PO10 to prioritize coverage over the occipital lobe. To monitor eye movements and blinks, EOG was recorded using four electrodes, two of which were placed above and below the right eye, and the other two were placed laterally to the left and right lateral canthi.

Data Analysis

Behavioral Analysis

We analyzed the behavioral responses (key presses to indicate the orientation of the target stimulus) that occurred between 300 and 1500 msec after the onset of target events. First, we assessed participants' ability to detect the targets, given the novel continuous stimulus presentation paradigm we implemented here. To do so, we classified responses as hits (participant responded within the response window by pressing any of the four arrow keys) and false alarms (participant pressed one of the four keys outside the response window). To quantify target detection performance, we used a modified calculation of observer sensitivity d' (Green & Swets, 1966) that yields an unbiased estimate in fast paced or continuous paradigms (Bendixen & Andersen, 2013), in which participants may respond continuously, as opposed to making a forced choice after each stimulus presentation. Under such circumstances, the denominator of the false alarm rate is ill-defined, as there either is no discrete number of nontargets or the rate at which nontargets are presented may be well beyond the response frequency of observers. To deal with this problem, the false alarm rate (f) is computed by dividing the number of false alarms (F) by the total length of time in which responses are recorded (T_S) divided by the length of the time-window after each target in which responses are classified as hits (T_R) minus the number of targets (N_T). To address the issue of infinite values in the cumulative normal distribution when the hit-rate h or the false-alarm rate f equals 0 or 1, the log-linear correction recommended by Hautus (1995) was applied (half a hit/false alarm is added to the observations). The resulting formula for the false alarm rate f is as follows:

$$f = \frac{F + 0.5}{\frac{T_S}{T_R} - N_T + 1} \tag{2}$$

The sensitivity index d' was calculated using the following standard formula:

$$d' = Z(h) - Z(f) \tag{3}$$

To quantify target identification performance, the mean proportion of correct responses was calculated for each condition by dividing the number of correct responses by the total number of target events.

EEG Preprocessing and Analysis

EEG data were processed using the EEGLAB toolbox (Delorme & Makeig, 2004) together with custom written routines in MATLAB. Epochs were extracted from all trials from 0 to 4000 msec after onset of the flickering stimuli and detrended (removal of mean and linear drifts). Epochs with eye movements or blinks were rejected from further analysis, and all remaining epochs were subsequently subjected to an automated procedure for artifact rejection and correction based on statistical parameters of the data (Junghöfer, Elbert, Tucker, & Rockstroh, 2000). On average, 71.3% (Experiment 1) and 71.4% (Experiment 2) of all epochs remained after artifact correction. All remaining epochs were averaged separately for each of the eight flanker distance conditions, and these averages were then subjected to a scalp current density ($\lambda = 10^{-5}$, m = 4, 50 iterations) transformation (Perrin, Pernier, Bertrand, & Echallier, 1989; Pernier, Perrin, & Bertrand, 1988). Scalp current density transforms differ from scalp potentials in that they are reference free, offer a higher spatial resolution, and better correspond with underlying cortical generators (Kayser & Tenke, 2005).

To quantify SSVEP amplitudes, these trial averages were subjected to a Fourier transform. The first 500 msec after the onset of the stimulus display were excluded from this calculation to allow for the SSVEP to build up. Five electrodes

with the highest SSVEP amplitudes averaged across all different target–flanker distances (including the no flanker condition) and participants were selected for each target flicker frequency (10 and 12 Hz) separately. SSVEP amplitudes were averaged across these five electrodes and subsequently rescaled. This rescaling was performed to account for differences in overall SSVEP magnitude between different participants and frequencies (Adamian & Andersen, 2024). Rescaled amplitudes N_{pfc} were calculated by dividing amplitudes A_{pfc} by the mean amplitude across conditions (c) for each participant (p) and each frequency (f) separately (Andersen, Fuchs, & Müller, 2011):

$$N_{pfc} = \frac{A_{pfc}}{\sum \left(A_{pc}\right)} \tag{4}$$

After rescaling, SSVEP amplitudes were collapsed across the two frequencies (i.e., targets).

Curve Fitting of Behavioral and EEG Data

To estimate critical spacing in Experiment 1, we fitted a cumulative Gaussian function to the mean proportion correct data and target-elicited SSVEP amplitudes as a function of flanker distance (excluding the no flanker condition). SSVEP amplitudes were noisier than the proportion correct data, which precluded fitting curves to individual participant's SSVEP data. Therefore, curve fits were performed on the group mean proportion correct and SSVEP amplitude data. The cumulative Gaussian is given by the following equation (Strasburger, 2001; Wichmann & Hill, 2001):

$$y = c + \frac{(\lambda - c)}{2} erfc\left(\frac{-b\,(x - a)}{\sqrt{2}}\right) \tag{5}$$

In this equation, y is proportion correct or target-elicited amplitude, x is the flanker distance, c is the lower asymptote, λ is the upper asymptote, b is the slope of the curve, a is the midpoint of the curve, and *erfc* is the complementary error function. For SSVEP data, the lower asymptote and the upper asymptote were constrained between half of the minimum amplitude across all conditions and to the maximum amplitude across all conditions. For behavioral data, all parameters were constrained to be nonnegative ($\geq$0) and the upper asymptote was constrained to a maximum of 1. In addition, for both SSVEP and behavioral data, the midpoint of the curve was constrained between the minimum and maximum flanker distance (1.7–5.1); and the slope was constrained between 0 and 10.

The critical spacing x_{cs} is commonly defined as the distance at which performance reaches 90% of the asymptote (Scolari et al., 2007):

$$x_{cs} = a + \frac{norminv\left(\frac{0.9\lambda - c}{\lambda - c}\right)}{b} \tag{6}$$

Here, *norminv* is the inverse of the normal cumulative distribution.

To estimate the sampling distribution of the critical spacings calculated based on proportion correct data and target-elicited SSVEP amplitudes, we used a resampling approach in which 1000 new samples with the original sample size were drawn with replacement from the original data set. Curve fitting was applied to the mean of each resample, and the corresponding critical spacing was then derived. To assess the quality of the fits, the coefficient of determination (r^2) and the adjusted r^2 (r^2_{adj}) were calculated for both the proportion correct and SSVEP data. The resulting critical spacing distributions were then used to calculate the medians and 95% confidence intervals of the critical spacings and of their difference.

Statistical Analysis

Behavioral (d' and proportion correct) and neural measures (target-elicited SSVEP amplitudes) were separately subjected to a one-way repeated-measures ANOVA in Experiment 1 (eight flanker distances including no flanker condition) and a two-way repeated-measures ANOVA in Experiment 2 with factors Flanker Distance (four flanker distances including no flanker condition) and Target–Flanker Similarity (similar and dissimilar). In addition, we computed Bayes Factors to assess the strength of evidence supporting or rejecting the effects of flanker distance (Experiment 1 and 2) and target–flanker similarity (Experiment 2). We used t tests to compare the behavioral and neural measures between successive flanker distances (Experiments 1 and 2) and flanker contrast conditions using Bonferroni–Holm correction for multiple comparisons.

RESULTS

Behavioral Data

Crowding leads to a failure of target identification, not detection (Petrov, Popple, & McKee, 2007; Pelli et al., 2004; Levi, Hariharan, & Klein, 2002). Unlike typical forced-choice paradigms commonly employed in psychophysical experiments, our two experiments employed a task in which participants identified target stimuli embedded in continuous stimulation. This allows for errors in both target detection and identification, and it is therefore necessary to assess both separately to verify that error responses actually reflect crowding (i.e., failures to identify) as opposed to detection errors.

In both experiments, only few false alarms and misses occurred, yielding very high detection performance as quantified via d' (Figures 2A and 3A). In Experiment 1, detection d' was independent of flanker distance, $F(7, 104) = 0.33$, $p = .87$, $\eta^2 = .02\%$, with the Bayes Factor providing very strong evidence against an effect of flanker distance ($BF_{10} = 0.032$). In Experiment 2, there was no effect of Flanker Distance, $F(3, 51) = 0.16$, $p = .92$, $\eta^2 = .65\%$; Similarity, $F(1, 17) = 0.01$, $p = .91$, $\eta^2 = .004\%$; or their interaction, $F(3, 51) = 0.44$, $p = .72$, $\eta^2 = .65\%$, on

detection d', and the Bayes Factor provided moderate evidence for the null hypothesis, with $BF_{10} = 0.14$ for flanker distance, $BF_{10} = 0.23$ for similarity, and strong evidence for the null hypothesis $BF_{10} = 0.03$ for the full model including interactions.

In Experiment 1, proportion correct decreased with decreasing flanker distance from the target, $F(7, 104) = 104.22, p < .001, \eta^2 = 88.91\%$ (Figure 2B). Pairwise comparisons between neighboring flanker distances revealed significant decreases between most pairs (1.7° vs. 2°: $t(13) = 4.07, p = .001$; 2° vs. 2.5°: $t(13) = 8.85, p < .001$; 2.5° vs. 3°: $t(13) = 4.22, p = .001$; 3° vs. 3.5°: $t(13) = 4.37, p < .001$; no flanker vs. 5.1°: $t(13) = 4.15, p = .001$) as flankers approached the target. RTs for correct responses exhibited a marked increase with decreasing target–flanker distance, $F(7, 104) = 28.70, p < .001, \eta^2 = 68.83\%$ (Figure 2C). Pairwise comparisons between neighboring flanker distances revealed significant increases at 5.1° spacing versus no flanker: $t(13) = -4.62, p < .001$.

In Experiment 2, both flanker distance (three distances plus no flanker condition) and similarity (similar vs. dissimilar) were manipulated. Proportion correct decreased with decreasing flanker distance, $F(3, 51) = 86.15, p < .001, \eta^2 = 48.41$ (Figure 3B), and this effect was magnified in the similar condition (Flanker Distance × Similarity: $F(3, 51) = 64.90, p < .001, \eta^2 = 17.04\%$; Similarity: $F(1, 17) = 148.13, p < .001, \eta^2 = 18.42$). RTs for correct responses (Figure 3C) increased with decreasing flanker distance, $F(3, 51) = 68.40, p < .001, \eta^2 = 50.40\%$. RTs were faster in the dissimilar condition, $F(1, 17) = 52.74, p < .001, \eta^2 = 16.74\%$, and there was a significant Flanker Distance × Similarity interaction, $F(3, 51) = 11.09, p < .001, \eta^2 = 5.90\%$, mainly due to the fact that the target–flanker similarity conditions were identical when there were no flankers.

Target-elicited SSVEP Amplitudes

The group average SSVEP amplitude spectrum and topographical maps averaged across all participants and conditions are displayed in Figure 2D and E. A one-way ANOVA indicated significant differences in target SSVEP amplitudes across target–flanker distances, $F(7, 104) = 15.26, p < .001, \eta^2 = 53.99\%$. Notably, there was a very pronounced drop in SSVEP amplitudes between the no flanker and the

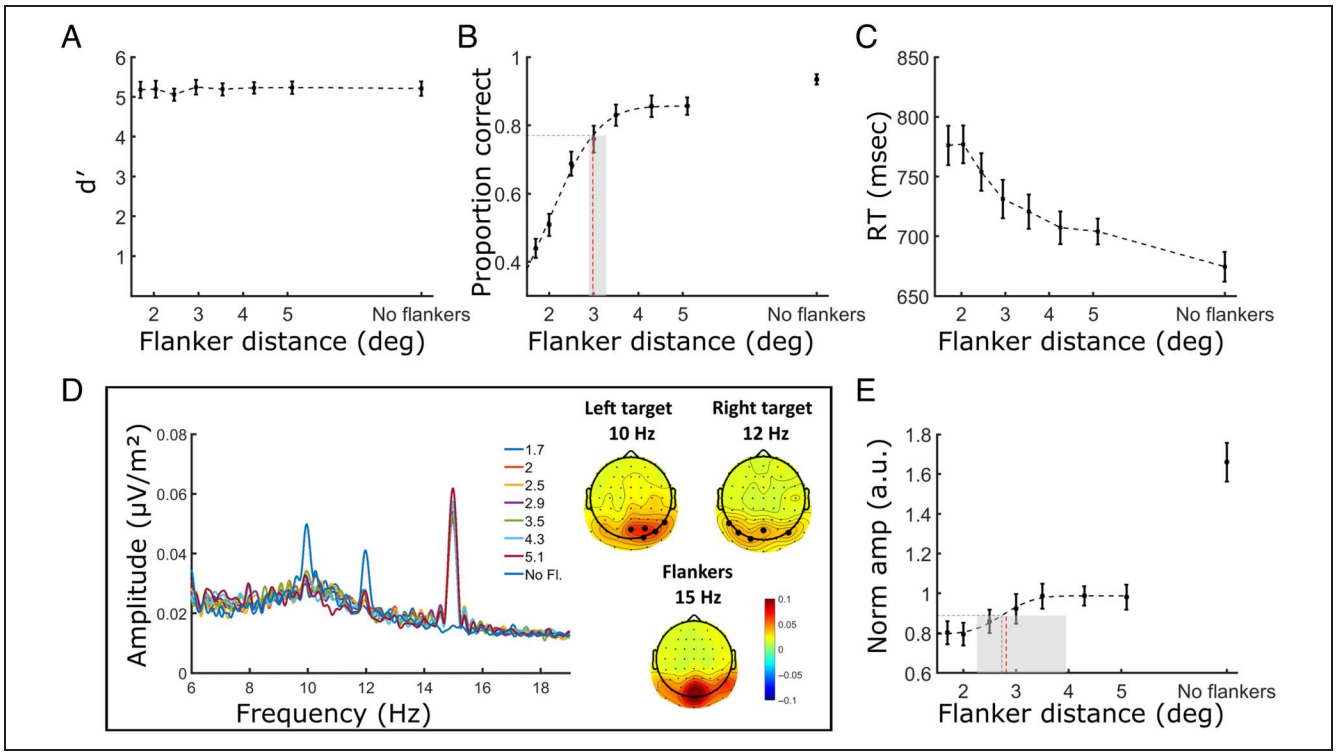

Figure 2. Behavioral and electrophysiological results in Experiment 1. (A) Average d' across participants as a function of target–flanker distance is plotted. Error bars represent *SEM*. (B) Average proportion correct in different target–flanker distances fitted with a Gaussian function. Ninety percent of the asymptote indicated as the critical spacing. Median (red dotted line) and 95% confidence intervals (gray area) of the critical spacings based on 1000 bootstrapped means. (C) Average RT in correct trials across participants. (D) Grand-average amplitude spectrum obtained by Fourier transform separately for each condition collapsed across occipital electrodes (P04, P08, P6, CP6, P8, P03, P07, P5, CP5, P7 Oz, POz, O2, Iz, and O1). Amplitudes peak at stimulation frequencies 10, 12, and 15 Hz; however, these peaks are more pronounced when stimulus-specific electrodes are chosen. Topographic maps of SSVEP amplitudes for each stimulus at stimulation frequencies averaged across all subjects and conditions (electrode positions chosen for analysis indicated with circles). (E) Average normalized target-related SSVEP amplitudes from five highest amplitude electrodes for each frequency separately, fitted identically to the behavioral data with critical spacing (black dotted line). Median (red dotted line) and 95% confidence intervals (gray area) of the critical spacings based on 1000 bootstrapped means.

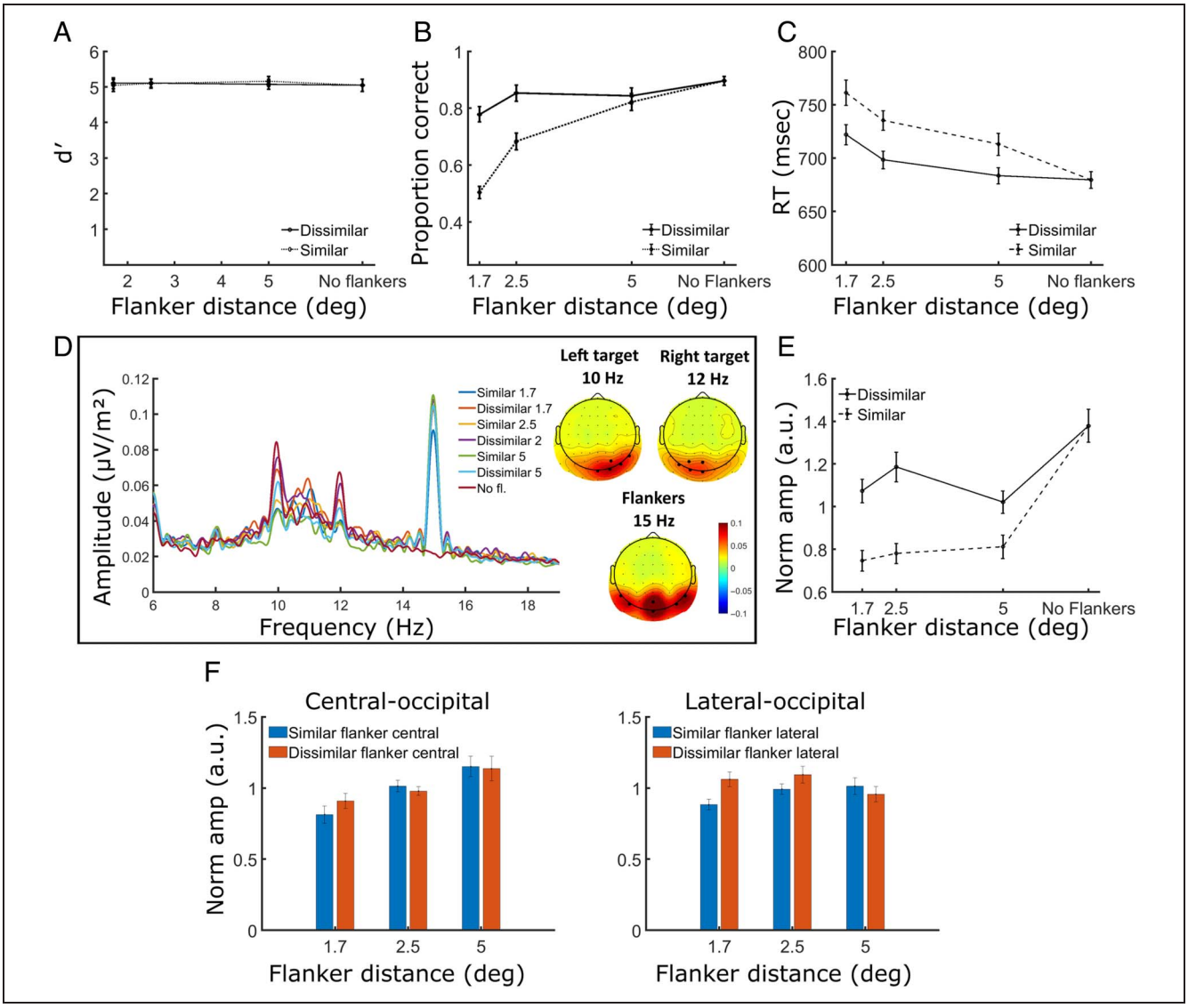

Figure 3. Behavioral and electrophysiological results in Experiment 2. (A) Average d' across participants as a function of target–flanker distance is plotted for each similarity condition; error bars represent *SEM*. (B) The proportion correct as a function of target–flanker distance. (C) Average RT in correct trials across participants. (D) Grand-average amplitude spectrum obtained by Fourier transform separately for each condition collapsed across occipital electrodes (P04, P08, P6, CP6, P8, P03, P07, P5, CP5, P7 Oz, POz, O2, Iz, and O1). Amplitudes peak at simulation frequencies 10, 12, and 15 Hz; however, these peaks are more pronounced when stimulus-specific electrodes are chosen. Topographic maps of SSVEP amplitudes for each stimulus at stimulation frequencies averaged across all subjects and conditions (electrode positions chosen for analysis indicated with circles). (E) Average normalized target-related SSVEP amplitudes from five highest amplitude electrodes for each frequency separately. (F) Flanker-elicited SSVEP amplitudes separately for central-occipital and lateral-occipital electrode positions in different target–flanker distances with *SEM*. Note that it is not meaningful to compare flanker-elicited neural responses across target–flanker distances, because they are confounded with flanker locations (i.e., eccentricities).

largest flanker distance conditions, $t(13) = 5.29, p < .001$, CI [0.40, 0.95].

In Experiment 2, target-elicited SSVEP amplitudes also decreased with decreasing flanker distance, $F(3, 51) = 13.23$, $p < .001$, $\eta^2 = 29.26\%$. SSVEP amplitudes were lower when the targets were similar to the flankers compared with when they were dissimilar, $F(1, 17) = 28.92$, $p < .001$, $\eta^2 = 10.19\%$. The reduction in target amplitudes as a function of target–flanker distance was greater in the similar condition compared with the dissimilar condition (interaction: $F(3, 51) = 6.57, p < .001$, $\eta^2 = 4.73\%$).

Critical Spacing

Cumulative Gaussian curve fits to proportion correct and target-elicited SSVEP amplitudes averaged across participants produced excellent fits (proportion correct: $r^2 = .995$, $r^2_{adj} = 0.99$; SSVEPs: $r^2 = .99$, $r^2_{adj} = 0.98$). The resultant estimates of critical spacing were very similar for proportion correct (2.99°) and target-elicited SSVEP amplitudes (2.73°). We employed a bootstrap approach to obtain estimates of variability of these estimates and their difference. As the pattern in SSVEPs was noisier than in the behavioral data, approximately 5% of the bootstrapped

samples did not yield a valid estimate of critical spacing and had to be excluded from our estimates of mean and 95% confidence intervals. The resulting estimates for proportion correct (median = 2.98, 95% CI: [2.89, 3.28]; Figure 2B) and SSVEP amplitudes (median = 2.81, 95% CI: [2.26, 3.95]; Figure 2E) exhibited substantial overlap, and the distribution of the difference between both included zero (median = 0.14, 95% CI: [−1.05, 0.96]); that is, it did not provide evidence for a difference.

Flanker-elicited SSVEP Amplitudes

An analysis of flanker-elicited SSVEP amplitudes across flanker distances would not yield unambiguously interpretable results in either experiment, as such comparisons would confound flanker position and distance to the target. Therefore, we exclusively compared flanker-elicited SSVEP amplitudes between the similar and dissimilar conditions in Experiment 2 for each flanker distance separately. Consistent with previous SSVEP experiments in which large symmetric stimuli were presented, the topography of flanker-elicited SSVEP amplitudes exhibited central and lateral peaks (Figure 3D), which most likely reflect activity in early (V1–V3) and later (MT, LOC) visual areas (Andersen, Müller, & Martinovic, 2012). Accordingly, flanker-elicited SSVEP amplitudes were analyzed for both clusters separately. At central electrodes, flanker-elicited SSVEP amplitudes did not differ between the similar and dissimilar conditions (1.7°: $t(17) = -2.05$, $p = .06$; 2.5°: $t(17) = 0.84$, $p = .40$; 5°: $t(17) = 0.41$, $p = .68$). At lateral-occipital electrodes, flanker-elicited SSVEP amplitudes were larger in the dissimilar condition than in the similar condition at the closest flanker distance (1.7°: $t(17) = -3.78$, $p = .001$), but there was no effect at the furthest flanker distance (2.5°: $t(17) = -1.31$, $p = .21$; 5°: $t(17) = 1.10$, $p = .28$).

DISCUSSION

In two experiments, we examined the hypothesis that suppressive interactions in visual processing of nearby stimuli might reflect a neural mechanism behind the breakdown of object recognition in visual crowding. We examined target identification performance and cortical processing of targets and flankers as a function of the distance (Experiments 1 and 2) and similarity (Experiment 2) between them. Both target identification as well as target-elicited SSVEP amplitudes are reduced as the distance between targets and flankers reduces (Experiments 1 and 2). However, this reduction does not occur when targets and flankers are dissimilar (Experiment 2). Correspondingly, dissimilar flankers elicited higher amplitudes at lateral-occipital electrodes at closer spacings than similar flankers, underlining the mutually suppressive interactions between target and flanker stimuli. Interestingly, the critical spacing estimates for proportion correct and target-elicited SSVEPs yield similar results. Taken together, these findings suggest that behavioral measures of crowding and the target-elicited SSVEPs here may reflect the same phenomenon. The study thus connects crowding to mutual interference between target and flanker processing in visual cortex and highlights the utility of SSVEPs as a tool to examining the cortical processing of multiple objects in the visual field over different spatial scales.

The similar critical spacing estimates for proportion correct and target-elicited SSVEPs reinforce the idea that both behavioral and electrophysiological measures capture the same underlying neural process. This finding suggests that SSVEPs could serve as a neural index for assessing the impact of crowding on object recognition in visual cortex and aligns with earlier studies showing that crowding involves spatial suppression in visual cortex (Millin et al., 2014; Anderson et al., 2012; Fang & He, 2008).

Target-elicited SSVEP amplitudes exhibited a marked suppression relative to the no-flanker condition even when flankers were placed at the furthest spacing. This pattern was especially pronounced in Experiment 1 and occurred despite SSVEP amplitudes seemingly reaching an asymptote at smaller spacings (Figure 2E). A similar pattern was observed for behavioral data (proportion correct responses; Figure 2B). Neither result was predicted, and in the following, we offer a speculative interpretation of these two effects.

The dramatic drop in target-elicited SSVEP amplitudes when flankers were present reflects flanker interference with target processing at large distances beyond the critical spacing. The existence of such long-range flanker interference is consistent with our previous study (Soo et al., 2018), which found large variations of the critical spacing ranging from 18% to 86% of the target eccentricity across different stimulus conditions. We speculate that such long-range interference from flankers on visual target processing is inherently present but only starts to manifest as behavioral errors in target identification once it reaches a certain strength at the critical spacing. The critical spacing is a function of multiple properties such as display duration (Soo et al., 2018; Tripathy et al., 2014; Tripathy & Cavanagh, 2002; Kooi et al., 1994), flanker and target contrast (Soo et al., 2018; Rashal & Yeshurun, 2014), backward masking (Vickery et al., 2009), pop-out (Kennedy & Whitaker, 2010; Põder & Wagemans, 2007; Scolari et al., 2007; Chung et al., 2001; Kooi et al., 1994; Nazir, 1992; Andriessen & Bouma, 1976), and flanker preview (Soo et al., 2018; Scolari et al., 2007; Watson & Humphreys, 1997), and our findings suggest that manipulations of these factors should modulate suppressive interactions in SSVEP amplitudes accordingly.

In addition, behavioral data in both of our experiments may have been affected by response competition between targets and flankers, as these had the same shapes but with randomly varied orientations. Response competition is commonly observed in conflict tasks such as the Simon (Simon, 1969), Stroop (Stroop, 1935), and Eriksen flanker (Eriksen & Eriksen, 1974) tasks. Such response selection

conflicts have been shown to modulate crowding (Reuther & Chakravarthi, 2020). Three specific factors in our experiments may have enhanced this response competition and led to error responses independent of target–flanker spacing (see Figure 2B: the asymptote is clearly below 1): First, the bilateral display with targets randomly occurring on the left or right side prevented participants from focusing attention strongly on the target location; second, we employed an inner flanker, which was at least as recognizable as the target itself due to its lower eccentricity (Papadaki, Chakravarthi, & Andersen, 2024); third, the continuous nature of the task may have induced participants to respond faster and commit errors. Although crowding was most likely absent at the furthest spacings and the no flanker condition, response competition would only be fully abolished in the no flanker condition leading to above asymptote performance. Response competition would however not have affected SSVEP amplitudes in our paradigm, as these were mainly driven by the nontarget placeholders and reflect visual stimulus processing rather than response selection.

Target detection performance was very high and unaffected by manipulations of target–flanker distance or flanker similarity in both of our experiments. This is in accordance with previous studies that have shown that crowding compromises target identification but not target detection (Petrov et al., 2007; Pelli et al., 2004; Levi et al., 2002). Hence, despite target stimuli being embedded in a continuous display and task in our paradigm, behavioral responses reflect a valid measure of crowding.

The alleviation of the interference caused by flankers when they are dissimilar to the target is in accordance with the well-established observation of the effect of similarity on crowding (Soo et al., 2018; Põder & Wagemans, 2007; Scolari et al., 2007; Chung et al., 2001; Andriessen & Bouma, 1976). We found that the neural signature of target–flanker interference in such situations closely matches the behavioral effect, with a reduction in flanker-induced interference at close distances when target–flanker polarity is dissimilar. This dissimilarity advantage effect has been previously explained by feature-specific filtering or interference (Pelli & Tillman, 2008; Pelli et al., 2004; Kooi et al., 1994), or grouping (Herzog et al., 2015; Manassi et al., 2012).

Our findings can be interpreted in the context of the biased competition model of attention (Desimone, 1998; Desimone & Duncan, 1995). The reduction of target processing in the presence flankers, even when the latter are presented at the furthest distance where they are expected to be beyond the critical spacing of crowding, is in line with the proposition that processing resources are spread across the entire visual field for multiple simultaneously presented stimuli (Treue, 2003). Our evidence supports that all objects in the visual field compete for neuronal processing resources (Rolls & Tovee, 1995), possibly due to limitations in available resources (Martin, 1986). This competition for processing resources is influenced by bottom–up mechanisms (here, distance and similarity between targets and flankers). When target and flankers are similar, their overlapping neural representations lead to stronger competition, which is reflected in a reduction of target-elicited SSVEP amplitudes. Similarly, Beck and Kastner (2007) found that competition for neuronal resources, as quantified by suppression in V4, was reduced when stimuli were dissimilar in color and orientation. Participants in our two experiments were instructed to allocate voluntary attention to the target locations, but we did not manipulate top–down attentional allocation between conditions. Therefore, our findings are only informative with respect to bottom–up competitive stimulus interactions and investigating the effects of direct manipulations of attentional allocation on target-elicited SSVEPs in crowding remains an important task for future studies. Such future work will also be able to test the attentional hypothesis of crowding, according to which crowding is caused by coarse spatial resolution of attention (Fang & He, 2008; Intriligator & Cavanagh, 2001; He et al., 1996) or unfocused spatial attention (Strasburger, 2005; Strasburger, Harvey, & Rentschler, 1991).

In Experiment 1, we found comparable estimates of critical spacing derived from behavioral performance (target orientation proportion correct) and those derived from neural measures (target-elicited SSVEPs). As SSVEPs mainly reflect visual processing in V1 (Norcia et al., 2015), our findings suggest that at least part of crowding-related interference occurs in early visual areas. Previous literature suggests that there are two separate hierarchical processes leading to object recognition: object individuation and identification (Xu, 2009; Intriligator & Cavanagh, 2001). On the basis of this hierarchical separation, critical spacing estimated from the target-elicited SSVEP amplitudes in our data could depict the bottleneck of object individuation (Chakravarthi & Herbert, 2019; Intriligator & Cavanagh, 2001). Once objects are individuated during early visual processing, object recognition takes place at a later stage, which might be further affected by interference.

Although SSVEPs mainly reflect visual processing in early cortical areas, it is not clear whether and by how much SSVEPs are affected by later cortical areas (Norcia et al., 2015). In line with an early cortical locus of crowding, previous studies have also shown suppression in V1 (Chen et al., 2014; Millin et al., 2014; Blake, Tadin, Sobel, Raissian, & Chong, 2006). However, the suppression of the target-elicited SSVEP amplitudes that we observed does not necessarily originate from early visual cortex. In our paradigm, the targets and flankers were displayed for 4 sec, within which there were up to two 500-msec target events. Because stimuli were presented continuously, recurrent processing is likely to have taken place. Thus, activity or interference in later visual areas (with larger receptive fields) could have been fed back to early visual cortex (Andersen & Müller, 2010). This is consistent with previous reports in crowding in terms of behavior (Manassi &

Whitney, 2018; Soo et al., 2018), neuroimaging (Freeman, Donner, & Heeger, 2011), and modeling (Francis, Manassi, & Herzog, 2017). Therefore, although SSVEP amplitudes recorded in our experiments predominantly reflect activity in early visual areas, our findings are consistent with the proposal that crowding occurs at multiple levels of the visual hierarchy (Manassi & Whitney, 2018; Soo et al., 2018; Ronconi, Bertoni, & Marotti, 2016; Whitney & Levi, 2011).

Corresponding author: Leili Soo, Miguel Hernandez University of Elche Institute of Bioengineering, Edifici Vinalopo, Elche, Spain, e-mail: leilisoo@gmail.com.

Data Availability Statement

The mean files of the SSVEP and the proportion correct data for all conditions for both experiments and a brief explanation of the data and analysis will be available on Open Science Framework at the following link: https://osf.io/d59qe/.

Author Contributions

Leili Soo: Conceptualization Data curation; Formal analysis; Funding acquisition; Investigation; Methodology; Project administration; Resources; Software; Validation; Visualization; Writing—Original draft; Writing—Review & editing. Plamen A. Antonov: Data curation; Formal analysis; Writing—Review & editing. Ramakrishna Chakravarthi: Conceptualization; Formal analysis; Funding acquisition; Investigation; Methodology; Project administration; Resources; Software; Supervision; Validation; Writing—Review & editing. Søren K. Andersen: Conceptualization; Data curation; Formal analysis; Funding acquisition; Investigation; Methodology; Project administration; Resources; Software; Supervision; Validation; Writing—Review & editing.

Funding Information

This work was supported by the Biotechnology and Biological Sciences Research Council (https://dx.doi.org/10.13039/501100000268; grant number BB/J01446X/1).

Diversity in Citation Practices

Retrospective analysis of the citations in every article published in this journal from 2010 to 2021 reveals a persistent pattern of gender imbalance: Although the proportions of authorship teams (categorized by estimated gender identification of first author/last author) publishing in the *Journal of Cognitive Neuroscience* (*JoCN*) during this period were M(an)/M = .407, W(oman)/M = .32, M/W = .115, and W/W = .159, the comparable proportions for the articles that these authorship teams cited were M/M = .549, W/M = .257, M/W = .109, and W/W = .085 (Postle and Fulvio, *JoCN*, 34:1, pp. 1–3). Consequently, *JoCN* encourages all authors to consider gender balance explicitly when selecting which articles to cite and gives them the opportunity to report their article's gender citation balance.

REFERENCES

Adamian, N., & Andersen, S. K. (2024). Attentional modulation in early visual cortex: A focused reanalysis of steady-state visual evoked potential studies. *Journal of Cognitive Neuroscience*, *36*, 46–70. https://doi.org/10.1162/jocn_a_02070, PubMed: 37847846

Adrian, E. D., & Matthews, B. H. (1934). The interpretation of potential waves in the cortex. *Journal of Physiology*, *81*, 440–471. https://doi.org/10.1113/jphysiol.1934.sp003147, PubMed: 16994555

Albonico, A., Martelli, M., Bricolo, E., Frasson, E., & Daini, R. (2018). Focusing and orienting spatial attention differently modulate crowding in central and peripheral vision. *Journal of Vision*, *18*, 4. https://doi.org/10.1167/18.3.4, PubMed: 29677319

Andersen, S. K., Fuchs, S., & Müller, M. M. (2011). Effects of feature-selective and spatial attention at different stages of visual processing. *Journal of Cognitive Neuroscience*, *23*, 238–246. https://doi.org/10.1162/jocn.2009.21328, PubMed: 19702461

Andersen, S. K., & Müller, M. M. (2010). Behavioral performance follows the time course of neural facilitation and suppression during cued shifts of feature-selective attention. *Proceedings of the National Academy of Sciences, U.S.A.*, *107*, 13878–13882. https://doi.org/10.1073/pnas.100243610, PubMed: 20643918

Andersen, S. K., Müller, M. M., & Hillyard, S. A. (2012). Tracking the allocation of attention in visual scenes with steady-state evoked potentials. In M. I. Posner (Ed.), *Cognitive neuroscience of attention* (2nd ed., pp. 197–216). Guilford Press.

Andersen, S. K., Müller, M. M., & Martinovic, J. (2012). Bottom-up biases in feature-selective attention. *Journal of Neuroscience*, *32*, 16953–16958. https://doi.org/10.1523/JNEUROSCI.1767-12.2012, PubMed: 23175846

Anderson, E. J., Dakin, S. C., Schwarzkopf, D. S., Rees, G., & Greenwood, J. A. (2012). The neural correlates of crowding-induced changes in appearance. *Current Biology*, *22*, 1199–1206. https://doi.org/10.1016/j.cub.2012.04.063, PubMed: 22658599

Andriessen, J. J., & Bouma, H. (1976). Eccentric vision: Adverse interactions between line segments. *Vision Research*, *16*, 71–78. https://doi.org/10.1016/0042-6989(76)90078-x, PubMed: 1258390

Beck, D. M., & Kastner, S. (2005). Stimulus context modulates competition in human extrastriate cortex. *Nature Neuroscience*, *8*, 1110–1116. https://doi.org/10.1038/nn1501, PubMed: 16007082

Beck, D. M., & Kastner, S. (2007). Stimulus similarity modulates competitive interactions in human visual cortex. *Journal of Vision*, *7*, 19. https://doi.org/10.1167/7.2.19, PubMed: 18217834

Bendixen, A., & Andersen, S. K. (2013). Measuring target detection performance in paradigms with high event rates. *Clinical Neurophysiology*, *124*, 928–940. https://doi.org/10.1016/j.clinph.2012.11.012, PubMed: 23266090

Blake, R., Tadin, D., Sobel, K. V., Raissian, T. A., & Chong, S. C. (2006). Strength of early visual adaptation depends on visual awareness. *Proceedings of the National Academy of Sciences, U.S.A.*, *103*, 4783–4788. https://doi.org/10.1073/pnas.0509634103, PubMed: 16537384

Bouma, H. (1970). Interaction effects in parafoveal letter recognition. *Nature*, *226*, 177–178. https://doi.org/10.1038/226177a0, PubMed: 5437004

Bundesen, C., Habekost, T., & Kyllingsbæk, S. (2005). A neural theory of visual attention: Bridging cognition and neurophysiology. *Psychological Review*, *112*, 291–328. https://doi.org/10.1037/0033-295X.112.2.291, PubMed: 15783288

Chakravarthi, R., & Cavanagh, P. (2007). Temporal properties of the polarity advantage effect in crowding. *Journal of Vision*, *7*, 11. https://doi.org/10.1167/7.2.11, PubMed: 18217826

Chakravarthi, R., & Cavanagh, P. (2009). Recovery of a crowded object by masking the flankers: Determining the locus of feature integration. *Journal of Vision*, *9*, 4. https://doi.org/10.1167/9.10.4, PubMed: 19810785

Chakravarthi, R., & Herbert, A. (2019). Two's company, three's a crowd: Individuation is necessary for object recognition. *Cognition*, *184*, 69–82. https://doi.org/10.1016/j.cognition.2018.12.008, PubMed: 30576886

Chen, J., He, Y., Zhu, Z., Zhou, T., Peng, Y., Zhang, X., et al. (2014). Attention-dependent early cortical suppression contributes to crowding. *Journal of Neuroscience*, *34*, 10465–10474. https://doi.org/10.1523/JNEUROSCI.1140-14.2014, PubMed: 25100582

Chicherov, V., & Herzog, M. H. (2015). Targets but not flankers are suppressed in crowding as revealed by EEG frequency tagging. *Neuroimage*, *119*, 325–331. https://doi.org/10.1016/j.neuroimage.2015.06.047, PubMed: 26102568

Chicherov, V., Plomp, G., & Herzog, M. H. (2014). Neural correlates of visual crowding. *Neuroimage*, *93*, 23–31. https://doi.org/10.1016/j.neuroimage.2014.02.021, PubMed: 24582921

Chung, S. T., Levi, D. M., & Legge, G. E. (2001). Spatial-frequency and contrast properties of crowding. *Vision Research*, *41*, 1833–1850. https://doi.org/10.1016/s0042-6989(01)00071-2, PubMed: 11369047

Chung, S. T. L., & Tjan, B. S. (2007). Shift in spatial scale in identifying crowded letters. *Vision Research*, *47*, 437–451. https://doi.org/10.1016/j.visres.2006.11.012, PubMed: 17223153

Danilova, M. V., & Bondarko, V. M. (2007). Foveal contour interactions and crowding effects at the resolution limit of the visual system. *Journal of Vision*, *7*, 25.1–25.18. https://doi.org/10.1167/7.2.25, PubMed: 18217840

Delorme, A., & Makeig, S. (2004). EEGLAB: An open source toolbox for analysis of single-trial EEG dynamics including independent component analysis. *Journal of Neuroscience Methods*, *134*, 9–21. https://doi.org/10.1016/j.jneumeth.2003.10.009, PubMed: 15102499

Desimone, R. (1998). Visual attention mediated by biased competition in extrastriate visual cortex. *Philosophical Transactions of the Royal Society of London, Series B: Biological Sciences*, *353*, 1245–1255. https://doi.org/10.1098/rstb.1998.0280, PubMed: 9770219

Desimone, R., & Duncan, J. (1995). Neural mechanisms of selective visual attention. *Annual Review of Neuroscience*, *18*, 193–222. https://doi.org/10.1146/annurev.ne.18.030195.001205, PubMed: 7605061

Eriksen, B. A., & Eriksen, C. W. (1974). Effects of noise letters upon the identification of a target letter in a nonsearch task. *Perception & Psychophysics*, *16*, 143–149. https://doi.org/10.3758/BF03203267

Fang, F., & He, S. (2008). Crowding alters the spatial distribution of attention modulation in human primary visual cortex. *Journal of Vision*, *8*, 6. https://doi.org/10.1167/8.9.6, PubMed: 18831642

Flom, M. C., Heath, G. G., & Takahashi, E. (1963). Contour interaction and visual resolution: Contralateral effects. *Science*, *142*, 979–980. https://doi.org/10.1126/science.142.3594.979, PubMed: 14069233

Francis, G., Manassi, M., & Herzog, M. H. (2017). Neural dynamics of grouping and segmentation explain properties of visual crowding. *Psychological Review*, *124*, 483–504. https://doi.org/10.1037/rev0000070, PubMed: 28437128

Freeman, J., Chakravarthi, R., & Pelli, D. G. (2012). Substitution and pooling in crowding. *Attention, Perception, & Psychophysics*, *74*, 379–396. https://doi.org/10.3758/s13414-011-0229-0, PubMed: 22160819

Freeman, J., Donner, T. H., & Heeger, D. J. (2011). Inter-area correlations in the ventral visual pathway reflect feature integration. *Journal of Vision*, *11*, 15. https://doi.org/10.1167/11.4.15, PubMed: 21521832

Fuchs, S., Andersen, S. K., Gruber, T., & Müller, M. M. (2008). Attentional bias of competitive interactions in neuronal networks of early visual processing in the human brain. *Neuroimage*, *41*, 1086–1101. https://doi.org/10.1016/j.neuroimage.2008.02.040, PubMed: 18424083

Green, D. M., & Swets, J. A. (1966). *Signal detection theory and psychophysics*. Wiley.

Greenwood, J. A., Bex, P. J., & Dakin, S. C. (2009). Positional averaging explains crowding with letter-like stimuli. *Proceedings of the National Academy of Sciences, U.S.A.*, *106*, 13130–13135. https://doi.org/10.1073/pnas.0901352106, PubMed: 19617570

Hautus, M. J. (1995). Corrections for extreme proportions and their biasing effects on estimated values of d'. *Behavior Research Methods, Instruments, & Computers*, *27*, 46–51. https://doi.org/10.3758/BF03203619

He, D., Wang, Y., & Fang, F. (2019). The critical role of V2 population receptive fields in visual orientation crowding. *Current Biology*, *29*, 2229–2236. https://doi.org/10.1016/j.cub.2019.05.068, PubMed: 31231052

He, S., Cavanagh, P., & Intriligator, J. (1996). Attentional resolution and the locus of visual awareness. *Nature*, *383*, 334–337. https://doi.org/10.1038/383334a0, PubMed: 8848045

Herzog, M. H., Francis, G., & Clarke, A. (2019). *Understanding statistics and experimental design: How to not lie with statistics*. Springer. https://doi.org/10.1007/978-3-030-03499-3

Herzog, M. H., & Sayim, B. (2022). Crowding: Recent advances and perspectives. *Journal of Vision*, *22*, 15. https://doi.org/10.1167/jov.22.12.15, PubMed: 36383366

Herzog, M. H., Sayim, B., Chicherov, V., & Manassi, M. (2015). Crowding, grouping, and object recognition: A matter of appearance. *Journal of Vision*, *15*, 5. https://doi.org/10.1167/15.6.5, PubMed: 26024452

Hirsch, J., & Curcio, C. A. (1989). The spatial resolution capacity of human foveal retina. *Vision Research*, *29*, 1095–1101. https://doi.org/10.1016/0042-6989(89)90058-8, PubMed: 2617858

Intriligator, J., & Cavanagh, P. (2001). The spatial resolution of visual attention. *Cognitive Psychology*, *43*, 171–216. https://doi.org/10.1006/cogp.2001.0755, PubMed: 11689021

Jehee, J. F. M., Roelfsema, P. R., Deco, G., Murre, J. M. J., & Lamme, V. A. F. (2007). Interactions between higher and lower visual areas improve shape selectivity of higher level neurons—Explaining crowding phenomena. *Brain Research*, *1157*, 167–176. https://doi.org/10.1016/j.brainres.2007.03.090, PubMed: 17540349

Junghöfer, M., Elbert, T., Tucker, D. M., & Rockstroh, B. (2000). Statistical control of artifacts in dense array EEG/MEG studies. *Psychophysiology*, *37*, 523–532. https://doi.org/10.1111/1469-8986.3740523, PubMed: 10934911

Kastner, S., De Weerd, P., Desimone, R., & Ungerleider, L. G. (1998). Mechanisms of directed attention in the human

extrastriate cortex as revealed by functional MRI. *Science*, *282*, 108–111. https://doi.org/10.1126/science.282.5386.108, PubMed: 9756472

Kastner, S., & Ungerleider, L. G. (2001). The neural basis of biased competition in human visual cortex. *Neuropsychologia*, *39*, 1263–1276. https://doi.org/10.1016/s0028-3932(01)00116-6, PubMed: 11566310

Kayser, J., & Tenke, C. E. (2005). Trusting in or breaking with convention: Towards a renaissance of principal components analysis in electrophysiology. *Clinical Neurophysiology*, *116*, 1747–1753. https://doi.org/10.1016/j.clinph.2005.03.020, PubMed: 16000258

Keitel, C., Andersen, S. K., & Müller, M. M. (2010). Competitive effects on steady-state visual evoked potentials with frequencies in- and outside the α band. *Experimental Brain Research*, *205*, 489–495. https://doi.org/10.1007/s00221-010-2384-2, PubMed: 20711565

Keitel, C., Andersen, S. K., Quigley, C., & Müller, M. M. (2013). Independent effects of attentional gain control and competitive interactions on visual stimulus processing. *Cerebral Cortex*, *23*, 940–946. https://doi.org/10.1093/cercor/bhs084, PubMed: 22510530

Kennedy, G. J., & Whitaker, D. (2010). The chromatic selectivity of visual crowding. *Journal of Vision*, *10*, 15. https://doi.org/10.1167/10.6.15, PubMed: 20884564

Keshvari, S., & Rosenholtz, R. (2016). Pooling of continuous features provides a unifying account of crowding. *Journal of Vision*, *16*, 39. https://doi.org/10.1167/16.3.39, PubMed: 26928055

Kewan-Khalayly, B., Migó, M., & Yashar, A. (2022). Transient attention equally reduces visual crowding in radial and tangential axes. *Journal of Vision*, *22*, 3. https://doi.org/10.1167/jov.22.9.3, PubMed: 35921089

Kewan-Khalayly, B., & Yashar, A. (2022). The role of spatial attention in crowding and feature binding. *Journal of Vision*, *22*, 6. https://doi.org/10.1167/jov.22.13.6, PubMed: 36479947

Kim, T., & Pasupathy, A. (2024). Neural correlates of crowding in macaque area V4. *Journal of Neuroscience*, *44*, e2260232024. https://doi.org/10.1523/JNEUROSCI.2260-23.2024, PubMed: 38670806

Klem, G. H., Lüders, H. O., Jasper, H., & Elger, C. (1999). The ten-twenty electrode system of the International Federation. The International Federation of Clinical Neurophysiology. *Electroencephalography and Clinical Neurophysiology*, *52*, 3–6. PubMed: 10590970

Kooi, F. L., Toet, A., Tripathy, S. P., & Levi, D. M. (1994). The effect of similarity and duration on spatial interaction in peripheral vision. *Spatial Vision*, *8*, 255–279. https://doi.org/10.1163/156856894x00350, PubMed: 7993878

Lee, J., & Maunsell, J. H. R. (2009). A normalization model of attentional modulation of single unit responses. *PLoS One*, *4*, e4651. https://doi.org/10.1371/journal.pone.0004651, PubMed: 19247494

Levi, D. M. (2008). Crowding—An essential bottleneck for object recognition: A mini-review. *Vision Research*, *48*, 635–654. https://doi.org/10.1016/j.visres.2007.12.009, PubMed: 18226828

Levi, D. M., Hariharan, S., & Klein, S. A. (2002). Suppressive and facilitatory spatial interactions in peripheral vision: Peripheral crowding is neither size invariant nor simple contrast masking. *Journal of Vision*, *2*, 167–177. https://doi.org/10.1167/2.2.3, PubMed: 12678590

Levi, D. M., & Klein, S. A. (1986). Sampling in spatial vision. *Nature*, *320*, 360–362. https://doi.org/10.1038/320360a0, PubMed: 3960118

Levi, D. M., Klein, S. A., & Yap, Y. L. (1987). Positional uncertainty in peripheral and amblyopic vision. *Vision Research*, *27*, 581–597. https://doi.org/10.1016/0042-6989(87)90044-7, PubMed: 3660620

Luck, S. J., Chelazzi, L., Hillyard, S. A., & Desimone, R. (1997). Neural mechanisms of spatial selective attention in areas V1, V2, and V4 of macaque visual cortex. *Journal of Neurophysiology*, *77*, 24–42. https://doi.org/10.1152/jn.1997.77.1.24, PubMed: 9120566

Malania, M., Herzog, M. H., & Westheimer, G. (2007). Grouping of contextual elements that affect vernier thresholds. *Journal of Vision*, *7*, 1. https://doi.org/10.1167/7.2.1, PubMed: 18217816

Manassi, M., Sayim, B., & Herzog, M. H. (2012). Grouping, pooling, and when bigger is better in visual crowding. *Journal of Vision*, *12*, 13. https://doi.org/10.1167/12.10.13, PubMed: 23019118

Manassi, M., Sayim, B., & Herzog, M. H. (2013). When crowding of crowding leads to uncrowding. *Journal of Vision*, *13*, 10. https://doi.org/10.1167/13.13.10, PubMed: 24213598

Manassi, M., & Whitney, D. (2018). Multi-level crowding and the paradox of object recognition in clutter. *Current Biology*, *28*, R127–R133. https://doi.org/10.1016/j.cub.2017.12.051, PubMed: 29408262

Martin, G. (1986). Limits of visual resolution. *Nature*, *319*, 540. https://doi.org/10.1038/319540a0, PubMed: 3945340

Millin, R., Arman, A. C., Chung, S. T. L., & Tjan, B. S. (2014). Visual crowding in V1. *Cerebral Cortex*, *24*, 3107–3115. https://doi.org/10.1093/cercor/bht159, PubMed: 23833128

Moran, J., & Desimone, R. (1985). Selective attention gates visual processing in the extrastriate cortex. *Science*, *229*, 782–784. https://doi.org/10.1126/science.4023713, PubMed: 4023713

Morgan, S. T., Hansen, J. C., & Hillyard, S. A. (1996). Selective attention to stimulus location modulates the steady-state visual evoked potential. *Proceedings of the National Academy of Sciences, U.S.A.*, *93*, 4770–4774. https://doi.org/10.1073/pnas.93.10.4770, PubMed: 8643478

Nandy, A. S., & Tjan, B. S. (2007). The nature of letter crowding as revealed by first- and second-order classification images. *Journal of Vision*, *7*, 5. https://doi.org/10.1167/7.2.5, PubMed: 18217820

Nazir, T. A. (1992). Effects of lateral masking and spatial precueing on gap-resolution in central and peripheral vision. *Vision Research*, *32*, 771–777. https://doi.org/10.1016/0042-6989(92)90192-l, PubMed: 1413560

Norcia, A. M., Appelbaum, L. G., Ales, J. M., Cottereau, B. R., & Rossion, B. (2015). The steady-state visual evoked potential in vision research: A review. *Journal of Vision*, *15*, 4. https://doi.org/10.1167/15.6.4, PubMed: 26024451

Papadaki, D., Chakravarthi, R., & Andersen, S. K. (2024). Distinct spatial patterns of flanker interference differentiate visual crowding from flanker compatibility effects in the Eriksen task. *PsyArXiv*. https://doi.org/10.31234/osf.io/h8dsg

Pelli, D. G. (2008). Crowding: A cortical constraint on object recognition. *Current Opinion in Neurobiology*, *18*, 445–451. https://doi.org/10.1016/j.conb.2008.09.008, PubMed: 18835355

Pelli, D. G., Palomares, M., & Majaj, N. J. (2004). Crowding is unlike ordinary masking: Distinguishing feature integration from detection. *Journal of Vision*, *4*, 1136–1169. https://doi.org/10.1167/4.12.12, PubMed: 15669917

Pelli, D. G., & Tillman, K. A. (2008). The uncrowded window of object recognition. *Nature Neuroscience*, *11*, 1129–1135. https://doi.org/10.1038/nn.2187, PubMed: 18828191

Pernier, J., Perrin, F., & Bertrand, O. (1988). Scalp current density fields: Concept and properties. *Electroencephalography and Clinical Neurophysiology*, *69*, 385–389. https://doi.org/10.1016/0013-4694(88)90009-0, PubMed: 2450736

Perrin, F., Pernier, J., Bertrand, O., & Echallier, J. F. (1989). Spherical splines for scalp potential and current density mapping. *Electroencephalography and Clinical Neurophysiology*, *72*, 184–187. https://doi.org/10.1016/0013-4694(89)90180-6, PubMed: 2464490

Petrov, Y., Popple, A. V., & McKee, S. P. (2007). Crowding and surround suppression: Not to be confused. *Journal of Vision*, *7*, 12.1–12.9. https://doi.org/10.1167/7.2.12, PubMed: 18217827

Põder, E., & Wagemans, J. (2007). Crowding with conjunctions of simple features. *Journal of Vision*, *7*, 23.1–23.12. https://doi.org/10.1167/7.2.23, PubMed: 18217838

Rashal, E., & Yeshurun, Y. (2014). Contrast dissimilarity effects on crowding are not simply another case of target saliency. *Journal of Vision*, *14*, 9. https://doi.org/10.1167/14.6.9, PubMed: 25476716

Reuther, J., & Chakravarthi, R. (2020). Response selection modulates crowding: A cautionary tale for invoking top–down explanations. *Attention, Perception, & Psychophysics*, *82*, 1763–1778. https://doi.org/10.3758/s13414-019-01891-5, PubMed: 31797179

Reynolds, J. H., & Heeger, D. J. (2009). The normalization model of attention. *Neuron*, *61*, 168–185. https://doi.org/10.1016/j.neuron.2009.01.002, PubMed: 19186161

Rolls, E. T., & Tovee, M. J. (1995). Sparseness of the neuronal representation of stimuli in the primate temporal visual cortex. *Journal of Neurophysiology*, *73*, 713–726. https://doi.org/10.1152/jn.1995.73.2.713, PubMed: 7760130

Ronconi, L., Bertoni, S., & Marotti, R. B. (2016). The neural origins of visual crowding as revealed by event-related potentials and oscillatory dynamics. *Cortex*, *79*, 87–98. https://doi.org/10.1016/j.cortex.2016.03.005, PubMed: 27088616

Saarela, T. P., Westheimer, G., & Herzog, M. H. (2010). The effect of spacing regularity on visual crowding. *Journal of Vision*, *10*, 17. https://doi.org/10.1167/10.10.17, PubMed: 20884482

Scolari, M., Kohnen, A., Barton, B., & Awh, E. (2007). Spatial attention, preview, and popout: Which factors influence critical spacing in crowded displays? *Journal of Vision*, *7*, 7.1–7.23. https://doi.org/10.1167/7.2.7, PubMed: 18217822

Simon, J. R. (1969). Reactions toward the source of stimulation. *Journal of Experimental Psychology*, *81*, 174–176. https://doi.org/10.1037/h0027448, PubMed: 5812172

Soo, L., Chakravarthi, R., & Andersen, S. K. (2018). Critical resolution: A superior measure of crowding. *Vision Research*, *153*, 13–23. https://doi.org/10.1016/j.visres.2018.08.005, PubMed: 30240717

Strasburger, H. (2001). Converting between measures of slope of the psychometric function. *Perception & Psychophysics*, *63*, 1348–1355. https://doi.org/10.3758/bf03194547, PubMed: 11800461

Strasburger, H. (2005). Unfocused spatial attention underlies the crowding effect in indirect form vision. *Journal of Vision*, *5*, 1024–1037. https://doi.org/10.1167/5.11.8, PubMed: 16441200

Strasburger, H., Harvey, L. O., Jr., & Rentschler, I. (1991). Contrast thresholds for identification of numeric characters in direct and eccentric view. *Perception & Psychophysics*, *49*, 495–508. https://doi.org/10.3758/bf03212183, PubMed: 1857623

Strasburger, H., & Malania, M. (2013). Source confusion is a major cause of crowding. *Journal of Vision*, *13*, 24. https://doi.org/10.1167/13.1.24, PubMed: 23335321

Strasburger, H., Rentschler, I., & Jüttner, M. (2011). Peripheral vision and pattern recognition: A review. *Journal of Vision*, *11*, 13. https://doi.org/10.1167/11.5.13, PubMed: 22207654

Stroop, J. R. (1935). Studies of interference in serial verbal reactions. *Journal of Experimental Psychology*, *18*, 643. https://doi.org/10.1037/h0054651

Toet, A., & Levi, D. M. (1992). The two-dimensional shape of spatial interaction zones in the parafovea. *Vision Research*, *32*, 1349–1357. https://doi.org/10.1016/0042-6989(92)90227-a, PubMed: 1455707

Treue, S. (2003). Visual attention: The where, what, how and why of saliency. *Current Opinion in Neurobiology*, *13*, 428–432. https://doi.org/10.1016/s0959-4388(03)00105-3, PubMed: 12965289

Tripathy, S. P., & Cavanagh, P. (2002). The extent of crowding in peripheral vision does not scale with target size. *Vision Research*, *42*, 2357–2369. https://doi.org/10.1016/S0042-6989(02)00197-9, PubMed: 12350424

Tripathy, S. P., Cavanagh, P., & Bedell, H. E. (2014). Large crowding zones in peripheral vision for briefly presented stimuli. *Journal of Vision*, *14*, 11. https://doi.org/10.1167/14.6.11, PubMed: 25550071

Tripathy, S. P., & Levi, D. M. (1994). Long-range dichoptic interactions in the human visual cortex in the region corresponding to the blind spot. *Vision Research*, *34*, 1127–1138. https://doi.org/10.1016/0042-6989(94)90295-x, PubMed: 8184557

Vickery, T. J., Shim, W. M., Chakravarthi, R., Jiang, Y. V., & Luedeman, R. (2009). Supercrowding: Weakly masking a target expands the range of crowding. *Journal of Vision*, *9*, 12.1–12.15. https://doi.org/10.1167/9.2.12, PubMed: 19271922

Wallis, T. S., & Bex, P. J. (2011). Visual crowding is correlated with awareness. *Current Biology*, *21*, 254–258. https://doi.org/10.1016/j.cub.2011.01.011, PubMed: 21277208

Watson, D. G., & Humphreys, G. W. (1997). Visual marking: Prioritizing selection for new objects by top–down attentional inhibition of old objects. *Psychological Review*, *104*, 90–122. https://doi.org/10.1037/0033-295x.104.1.90, PubMed: 9009881

Whitney, D., & Levi, D. M. (2011). Visual crowding: A fundamental limit on conscious perception and object recognition. *Trends in Cognitive Sciences*, *15*, 160–168. https://doi.org/10.1016/j.tics.2011.02.005, PubMed: 21420894

Wichmann, F. A., & Hill, N. J. (2001). The psychometric function: I. Fitting, sampling, and goodness of fit. *Perception & Psychophysics*, *63*, 1293–1313. https://doi.org/10.3758/bf03194544, PubMed: 11800458

Wilkinson, F., Wilson, H. R., & Ellemberg, D. (1997). Lateral interactions in peripherally viewed texture arrays. *Journal of the Optical Society of America A*, *14*, 2057–2068. https://doi.org/10.1364/josaa.14.002057, PubMed: 9291601

Xu, Y. (2009). Distinctive neural mechanisms supporting visual object individuation and identification. *Journal of Cognitive Neuroscience*, *21*, 511–518. https://doi.org/10.1162/jocn.2008.21024, PubMed: 18510449

Yashar, A., Chen, J., & Carrasco, M. (2015). Rapid and long-lasting reduction of crowding through training. *Journal of Vision*, *15*, 15. https://doi.org/10.1167/15.10.15, PubMed: 26583278

Yeshurun, Y., & Rashal, E. (2010). Precueing attention to the target location diminishes crowding and reduces the critical distance. *Journal of Vision*, *10*, 16. https://doi.org/10.1167/10.10.16, PubMed: 20884481